A Compliant Optical Mount Design

Jeffrey M. Steele
John F. Vallimont
Brian S. Rice

Eastman Kodak Company
Rochester, New York

Gary J. Gonska

Allied-Signal Aerospace Corporation
Teterboro, New Jersey

ABSTRACT

A lens mount has been designed to accommodate both thermal excursions and severe dynamic loadings without introducing significant aberrations into the optic or incurring permanent alignment shifts. The mount was analyzed and tested over a wide range of environmental conditions and found to meet all of its performance goals. This paper illustrates, in detail, the methodology employed in the design of this mount assembly including manufacturability and performance analysis and testing.

1. INTRODUCTION

An optical lens mount was required to satisfy the following criteria:

> Withstand high (30 grms) random vibratory loading while maintaining alignment within 4 arc seconds tilt and 0.0001 inches decenter.
>
> Accommodate a 25°F temperature change without inducing significant aberrations into the optic.
>
> Fit within a constrained space envelope, with no obstruction of the optic.
>
> Be capable of simple alignment and assembly operations. Utilize Invar for the structure, RTV for the adhesive and fused silica for the optic.

The design of this mount was part of a concurrent design effort of a full optical system. The design process employed, including the manufacture, analysis and testing of a mount assembly breadboard, represented an example of a rigorous systems engineering approach to the design of an optical system subassembly. The design process included analysis and testing to support manufacturability and performance predictions. The design and analysis models, first developed for the breadboard assembly, were validated by the breadboard testing and used, almost simultaneously, in the design of the mounts for the full optical system.

In addition to providing data to support assignment of manufacturing tolerances the manufacture of the breadboard allowed manufacturing personnel an early opportunity to fine tune processes and equipment prior to assembly of the first full optical system.

Two trade studies were first performed to choose the best design concept; and a series of analyses and tests were performed to quantify the performance of the selected design concept prior to its incorporation into the full system design.

0-8194-0855-7/92/$4.00

2. TRADE STUDIES

The first of two trade studies was performed to evaluate several design concepts against the above criteria. These concepts included:

- o Round bipods attaching to the side of the optic.
- o Flat, blade bipods, attaching in a similar manner.
- o Tangential blade (leaf spring) flexures (Ref. 1 and 2).
- o Integral Ring concept.

The Integral Ring mount concept is shown in Figures 1 and 2. It consists of a box-section Invar ring with the top and bottom, inside corners cut away along 3 equally spaced arcs to form three curved "flexures". The fused silica optic is bonded to the flexure segments of the ring inside diameter using an RTV silicon rubber adhesive.

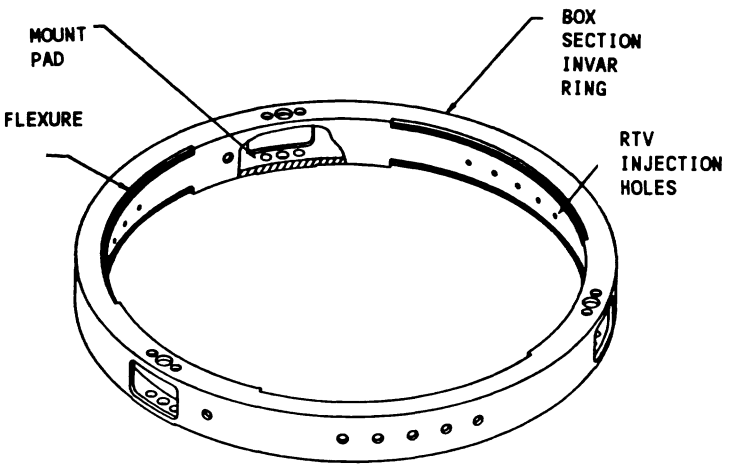

Figure 1 Integral Ring Concept

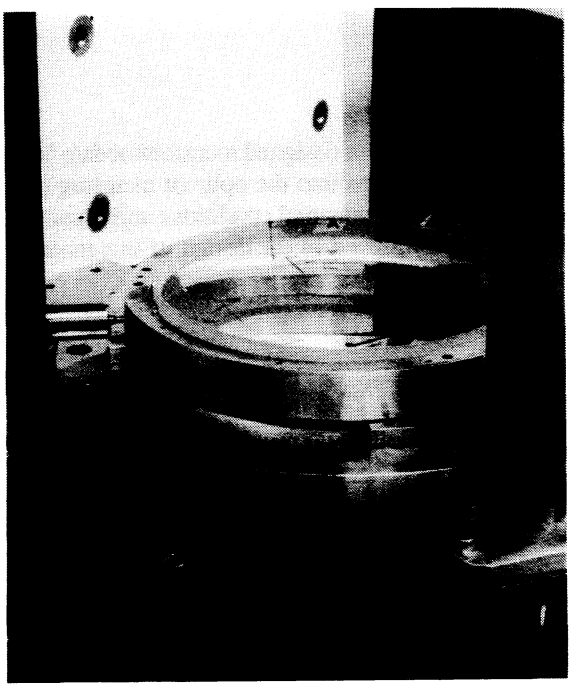

Figure 2 Assembled Mount on Alignment Tower

Table 1 gives the results of the trade study including the specific performance metrics used to evaluate each criteria. The results showed that the Integral Ring concept had the highest rigidity, lowest cost, and highest, but still acceptable, mount induced optic figure error. There is a direct and inverse relationship between mount rigidity and thermally induced figure error. The RTV adhesive has a coefficient of thermal expansion (CTE) of 400 microinch/in/°F which is about 1000 times higher than either the Invar ring (0.45 microinch/in/°F) or the fused silica optic (0.35 microinch/in/°F). Higher mount ring stiffness causes larger thermally induced aberrations in the optic, primarily power, trefoil and astigmatism, due to the reaction forces from the RTV expanding against the Invar mount ring. Higher mount ring stiffness, however, reduces dynamic stresses from vibration exposure and minimizes the risk of an optic shift due to Invar microyield.

A second trade study was conducted to determine the angular dimension of the RTV pad. Pad dimensions of 30° and 45° were evaluated to determine which size gave the optimum compliance balance between dynamic stress and thermally induced mount aberrations. Four analyses were performed to evaluate the 30° vs. 45° RTV pad sizes:

1) Thermoelastic analysis to calculate aberrations in the optic due to a 25°F temperature change.
2) 100G static loads applied in each of three directions to approximate peak dynamic loads.
3) 25 arc second mount pad tilt. Flat shims, used to correct tilt, of various thicknesses (up to a differential of 0.001 inch) under the three mounting pads will cause a twist in the mount ring and optical aberrations.

4) Natural frequencies as a measure of the assembly's resistance to vibration exposure.

Results of the pad size trade study are given in Table 2.

	ROUND BIPOD	BLADE BIPOD	TANGENT BLADE	INTEGRAL RING
1 VIBRATION SHIFT RISK				
1.1 NUMBER OF BOLTED CONNECTIONS	9 PER CELL	9 PER CELL	9 PER CELL	3 PER CELL
1.2 NATURAL FREQUENCY	180 Hz	180 Hz	198 Hz	212 Hz
1.3 STRESS RELAXATION, RTV	<0.0001 IN. DECENTER ACCEPTABLE	<0.0001 IN. DECENTER ACCEPTABLE	<0.0001 IN. DECENTER ACCEPTABLE	<0.0001 IN. DECENTER ACCEPTABLE
2 COST				
2.1 NUMBER OF INDIVIDUAL PARTS	7	4	4	1
2.2 SUBASSEMBLY ALIGNMENT REQUIRED	YES	YES	YES	NO
2.3 COMPLEXITY OF FINAL ASSEMBLY	HIGH	LOW	LOW	LOW
3 OPTICAL PERFORMANCE				
3.1 MOUNT INDUCED FIGURE ERROR WAVES, RMS	0.004 ACCEPTABLE	0.004 ACCEPTABLE	<0.001 ACCEPTABLE	0.006 ACCEPTABLE

Table 1 Optical Mount Design Trade Study Results

Thermoelastic and mount pad optical aberration analysis was performed using finite element analysis with MSC/NASTRAN®* (Figures 3 and 4) and the Kodak proprietary program, NASTRACT (Ref. 3). NASTRACT was used to decompose the surface displacements from the finite element analysis into the Zernike component aberrations.

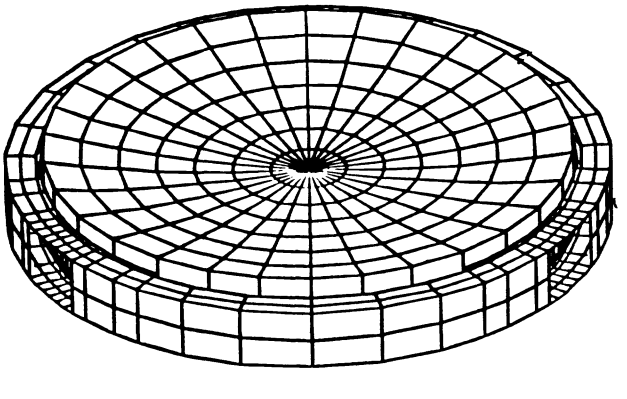

Figure 3 Detailed Finite Element Model

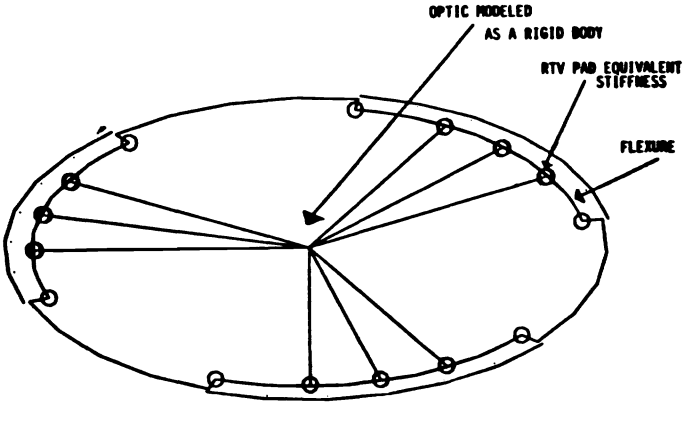

Figure 4 Simplified Finite Element Model

* MSC/NASTRAN is a product of the MacNeal Schwendler Corporation, Los Angeles California

The results shown in Table 2 show that the 45° pad size produced higher thermally induced aberrations than the 30° pad, although both were below 0.10 waves, rms, which was judged to be an acceptable limit. The dynamic stresses, at 100G, showed that the peak dynamic stress for the 30° pad was 21.9 KSI which exceeds the microyield lower limit for Invar of 15 KSI. This implies that there is a risk of microyield and permanent plastic deformation of the mount ring with the 30° pad. Peak stresses for the 45° pad were 15 KSI, at the lower end of the microyield range. The decision was made to use the 45° pad size in the final design.

THERMOELASTIC 25°F TEMPERATURE DELTA				
SURFACE FIGURE	30° Pad		45° Pad	
ERROR, WAVES	FRONT	BACK	FRONT	BACK
TOTAL	0.025	0.046	0.055	0.075
POWER REMOVED	0.013	0.013	0.028	0.027
ASTIGMATISM REM	0.013	0.013	0.028	0.027
TREFOIL REMOVED	0.001	0.001	0.001	0.001
MOUNT RING PAD TILT - 0.001" (25 ARCSEC)				
SURFACE FIGURE	30° Pad		45° Pad	
ERROR, WAVES	FRONT	BACK	FRONT	BACK
TOTAL	0.009	0.009	0.025	0.025
POWER REMOVED	0.009	0.009	0.025	0.025
ASTIGMATISM REM	0.001	0.001	0.003	0.003
TREFOIL REMOVED	0.001	0.001	0.003	0.003
PEAK STRESSES 100G LOADING				
MAX RING STRESS	21.9 KSI		15.0 KSI	
MAX RTV STRESS	220.0 PSI		150.0 PSI	
NATURAL FREQUENCIES				
AXIAL MODE	211 Hz		252 Hz	
ROCKING MODE	276 Hz		329 Hz	

Table 2 Results of Pad Size Trade Study

3. TESTING AND ANALYSES

Following the two trade studies, a breadboard of the optical mount assembly was designed, assembled and run through a series of analyses and tests. These analyses and tests were intended to characterize the performance of the mount through its assembly process and operating environments as it would be used in a full optical system.

Testing and analyses were performed to address the following parameters:

Manufacturability - Final alignment through adhesive bonding and optical aberrations due to adhesive cure shrinkage.

Thermal Sensitivity - Thermally induced optical aberrations, and thermally induced tilts due to isothermal and gradient conditions across the assembly.

Dynamic Response - Measurements and calculation were compared for static stiffness, natural frequencies and mode shapes, and dynamic random vibration response. Optic alignment shifts through vibration exposure were measured.

3.1 ALIGNMENT TESTS

OBJECTIVE :
The objective of the alignment tests was to measure alignment shifts which occurred during the bonding operation, thermal testing, and vibration testing; and to determine whether these shifts fall within allowable tolerances.

ALIGNMENT MEASUREMENTS PROCEDURE:
The decenter and tilt measurements were made using an autocollimating telescope, axicon, and dial indicator gages. The alignment measurements were taken prior to bonding of the optic, immediately after bonding, after a 7 day cure, at each phase of support hardware removal, and after thermal cycling and vibration testing.

The test sequence and measured shifts are listed in Table 3. The measurement resolution was 0.0001 inch for decenter and 1 arc second for tilt (See Figure 2). Both tilt and decenter were measured with an axicon. Redundant measurements were performed with an autocollimating telescope and decenter was measured with 0.0001 resolution dial indicators.

RESULTS:
Bonding: The alignment of the mirror after the bonding operation with respect to the mounting reference was 5 arc-seconds tilt and 0.0005" decenter. This was well within the manufacturing tolerance of 30 arc-seconds tilt and 0.003" decenter.

Thermal testing: After completion of the isothermal/non-isothermal test, the breadboard assembly was installed on the alignment tower. No measurable shift for either tilt of decenter could be detected.

Vibration testing: The alignment of the mirror was measured on the alignment tower after a vibration exposure of 3 minutes at 8.4 Grms input level. The measurements indicated a .0001" change in decenter and 3 arc seconds change in tilt. These values are at the limits of repeatability for removing the breadboard from the alignment tower, and remounting it on the tower. These shift numbers were acceptable and within the budgeted tolerance.

CONCLUSIONS :
The final alignment of the optic following bonding, and removal of the support equipment was well within the assembly tolerance, and did not require re-shimming or re-centering. There was no detectable permanent change as a result of the thermal testing. The shifts due to vibration testing were within acceptable limits.

3.2 ADHESIVE CURE INDUCED FIGURE ERROR

OBJECTIVE:
To determine the amount of figure error induced into the mirror during mounting due to support stress, RTV curing, manufacturing and assembly non-uniformities.

TEST DESCRIPTION:
The figure of the plano side of the optic was measured using a Fizeau interferometer before and after mounting, and the Pre-to-Post errors were then subtracted from each other to determine the induced errors. The two interferograms were subtracted on a point-by-point basis, and the Zernike polynomial terms were extracted from this difference map.

RESULTS:
The Pre-bond to Post-bond change in figure error was 0.013 waves, rms. This value was at the resolution limit of the interferometry. The allotted budget value for mounting induced figure errors was 0.050 waves, rms.

CONCLUSIONS:
The results showed that there was no significant figure error induced from assembly or RTV cure.

	AXICON TILT ARCSEC	AXICON DECENT. INCHES	AUTOCOLL. TILT ARCSEC	DIAL IND. DECENT. INCHES
PRE-POST BOND DELTA	0.7	0.0001	1.0	0.0002
THERMAL TEST DELTA	1.0	0.0001	1.0	0.0000
VIBRATION TEST DELTA	3.0	0.0000	2.5	0.0000

Table 3 Optic Alignment Shifts Through Assembly and Testing

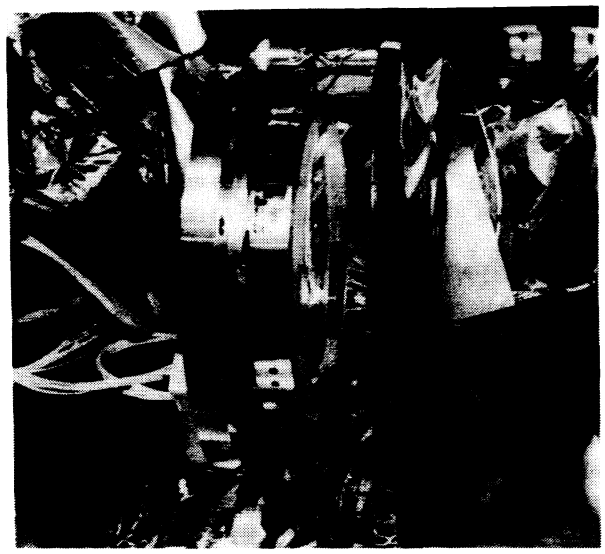

Figure 5 Thermal Test Configuration

3.3 THERMAL TESTS

OBJECTIVE:
To determine the wavefront and tilt sensitivity of the mounted optic to isothermal and non-isothermal (side to side gradients) temperatures, and to compare these sensitivities against calculated values.

TEST CONFIGURATION:
The optic mount assembly was assembled inside a thermal shroud in a vacuum chamber (see Figure 5). The shroud was heated to provide an isothermal environment for the different test temperatures. Heater tapes attached to the mounting ring provided the non-isothermal test gradients. Thermocouples were attached to the optic, mounting ring, interface plate, shroud, and vacuum chamber. A window in the vacuum chamber provided a port for interferometry to measure the wavefront and for an autocollimating telescope to measure the tilt of the optic.

TEST RESULTS:

ISOTHERMAL TEST:
The assembly was tested at 68, 85, 90, 95, and 105°F, and the wavefront values were subtracted from the pre-bonding measurements of the isolated optic, prior to assembly, taken at those temperatures (see Table 4). A figure change of 0.025 waves, rms was induced in the assembled optic by the temperature increase from the 68°F to 95°F. This value was compared to the predicted value of 0.055 waves, rms.

The tilt changes in the optic at the different temperatures were also measured (see Table 5). The tilt change from 68°F to 105°F was 1 arc second, the measurement resolution of the autocollimating telescope.

After the isothermal test, the figure and tilt of the optic was measured at 68°F. No permanent change (pre-post isothermal test) in either figure or alignment could be measured.

NON-ISOTHERMAL TEST: The optic mount assembly was brought to an isothermal temperature of 90°F, and a side-to-side gradient of 11.6°F was induced into the optic mounting ring using heater tapes. The gradient induced into the mounting ring was an order of magnitude greater than anticipated for actual use, to magnify errors to a measurable level. A figure change of 0.016 waves, rms was induced into the optic. A 1 arc second tilt was measured, as shown in Table 5.

WAVEFRONT INTERFEROMETRY TEST DATA
POST-BONDING THERMAL TEST OF ASSEMBLY
WAVEFRONT, WAVES RMS

TEST POST-BOND	TOTAL RMS	SAG REM	ASTIG REM	COMA REM	TREFOIL REM
ISOTHERMAL					
68°F	0.029	0.022	0.009	0.009	0.007
85°F	0.035	0.021	0.011	0.011	0.009
90°F	0.041	0.020	0.011	0.011	0.009
95°F	0.038	0.020	0.010	0.010	0.007
105°F	0.052	0.024	0.009	0.009	0.009
68°F	0.027	0.021	0.011	0.011	0.008
SIDE-SIDE GRADIENT					
7°F	0.044	0.024	0.010	0.010	0.008
11.6°F	0.046	0.019	0.015	0.012	0.012
0°F	0.029	0.025	0.011	0.011	0.011

Table 4 Thermal Figure Change Results

THERMAL TILT MEASUREMENTS

ISOTHERMAL TEMP °F	TILT ARCSEC	NON-ISOTHERM TEMP °F	TILT ARCSEC
68 AMB.	0	68 AMB.	0
85	0	7.0 GRAD.	1
90	1		
95	1	11.6 GRAD.	1
105	1		
68 AMB.	0	68 AMB.	0

Table 5 Thermal Tilt Results

After the non-isothermal temperature test, the optic was measured at 68°F. No permanent change in either figure or alignment (pre-post non-isothermal test) could be measured.

CONCLUSIONS:
ISOTHERMAL TEST:
The 0.025 waves rms figure error was less than the prediction. The 1 arc second tilt of the optic with respect to the mount is the limit of the measurement capability of the autocollimating telescope, and represents an acceptable tilt. There was no permanent tilt or figure changes.

NON-ISOTHERMAL TEST:
A Thermal gradient, which was an order of magnitude greater than required, across the optical mount induced a surface error of 0.016 waves, rms. This response is significantly less than the budget of 0.050 waves, rms.

3.4 STATIC DEFLECTION TESTS AND ANALYSES

OBJECTIVE:
The static deflection test was performed to compare the results of the detailed and simplified finite element models of the assembly against test results for static deflections in the radial and axial directions. This test was intended to provide a calibration for the two models with respect to the modeled stiffness of the mount ring and the effective stiffness of the RTV adhesive.

PROCEDURE:

Separate tests were performed, using 0.0001 inch resolution dial indicators, for radial and axial static deflections. Loadings to 40 lbf, in 10 lbf increments, were applied. A zero loading reading was taken at the end of the sequence to check for any permanent deflections.

All finite element calculations were performed with MSC/NASTRAN®

RESULTS:
Table 6 shows the load vs deflection for the test results and both the simplified and detailed finite element models. The results indicated that both finite element models had excellent correlation with the measured deflections in the axial direction. However, for the radial direction, that both finite element models under-predicted the deflections by 38%. A 38% difference in stiffness is consistent with a 11.3% difference in flexure thickness. The flexure nominal thickness is

0.065 inches the as-measured flexure thickness of the breadboard mount was 0.060 to 0.062. This difference would account for a 21% difference in stiffness, by itself. Furthermore, it is expected that finite element models tend to be over-stiff because they assume perfectly rigid connections, unless otherwise specified.

STATIC DEFLECTION TEST AND ANALYSIS

	TEST		ANALYSIS (DETAILED)		ANALYSIS (SIMPLIFIED)	
LOAD	RADIAL	AXIAL	RADIAL	AXIAL	RADIAL	AXIAL
LBF.	INCHES	INCHES	INCHES	INCHES	INCHES	INCHES
0.0	0.0000	0.0000	0.0000	0.0000	0.0000	0.0000
10.0	0.0001	0.0004	0.0001	0.0004	0.0001	0.0004
20.0	0.0002	0.0008	0.0001	0.0008	0.0001	0.0008
30.0	0.0003	0.0012	0.0002	0.0012	0.0002	0.0012
40.0	0.0004	0.0016	0.0003	0.0016	0.0002	0.0016
0.0	0.0000	0.0000	0.0000	0.0000	0.0000	0.0000

Table 6 Static Deflection Test and Analysis Data

CONCLUSIONS:
The correlation between the finite element models and the axial test measurements was very good. The correlation in the axial direction was excellent. The correlation in the radial direction was also very good and the difference can be attributed to the breadboard ring actual as-machined dimensions, which were at the lower bound of the thickness tolerance. This comparison gives an indication as to the range of variability to be expected across a population of mount rings.

3.5 DYNAMIC RESPONSE TESTS - MODAL TEST AND ANALYSES

OBJECTIVE:
To determine the natural frequencies and mode shapes of the mount assembly and compare measured frequencies against calculated frequencies for both finite element models. It is anticipated that the optic will behave as a rigid body vibrating against the mount ring via the stiffness of the flexures. There should be a total of six rigid body modes, although several of the higher modes may be outside the frequency range of interest (up to 2000 Hz).

PROCEDURE:
The modal survey test was performed by mounting a triaxial accelerometer at the center of the bottom (flat) side of the optic. An instrumented hammer was used to tap the optic and mount ring at 24 test points. See Figures 6 and 7. The test was performed with the Structural Measurement Systems, Inc. modal test system.

All finite element calculations were performed with the same models used for the static deflection analysis, using MSC/NASTRAN®.

RESULTS:
Table 7 gives the measured and calculated natural frequencies, and modal damping ratios from the modal survey test, the finite element analyses, and from the sine sweep test.

Figures 8 through 10 show the comparison of the calculated and measured mode shapes for modes 1 - 3. These results show that the first mode is an axial mode, the second mode is a rocking mode and the third mode is a transverse (radial direction) mode. Both the second and third modes are mode pairs, as predicted by the analysis. The test, as expected, could not separate the individual frequencies, which are theoretically identical.

NATURAL FREQUENCIES - ANALYSIS AND TEST

	MODAL TEST		SINE	ANALYSIS MODELS	
	FREQ.	DAMPING	SWEEP	DETAILED	SIMPLIFIED
MODE	Hz.	RATIO	FREQ, Hz	Hz.	Hz.
1	244	1.8%	256	253	246
2	309	4.0%	324	314	316
3	557	0.9%	591	592	647

Table 7 Natural Frequencies

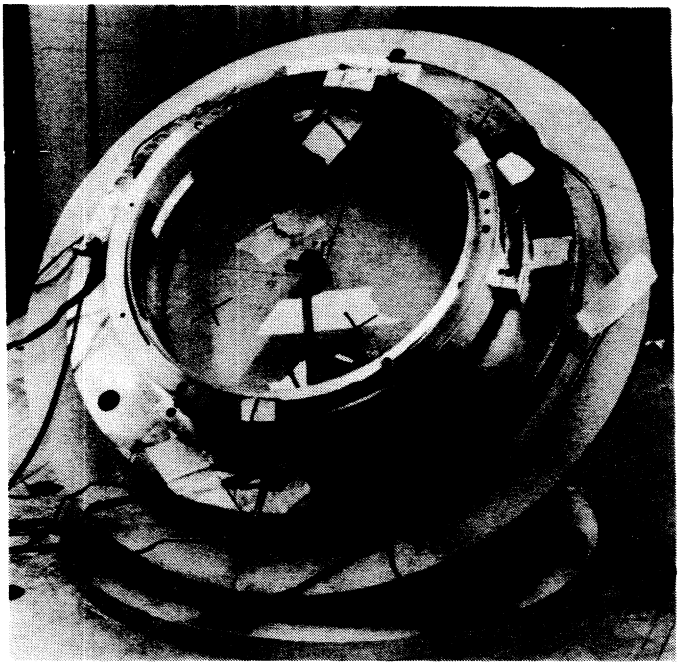

Figure 6 Vibration Test Configuration

The comparison of the modal test and analysis results show that the detailed model accurately predicted the test results for both radial and axial stiffness (modes 1 and 3), within 6% in frequency, and 13% in stiffness (where frequency is proportional to the square root of stiffness, assuming the mass of the optic is correct) for both cases. The comparison of the simplified model results with test data show that the simplified model is within 1% in frequency, and 2% in stiffness in the axial direction and 16% in frequency and 35% in stiffness in the radial direction.

The comparison of the finite element results against the modal test data is consistent with the results of the static deflection tests where the finite element model gave very good correlation for the axial direction, and over predicted the stiffness in the radial direction by 33%. This comparison is consistent with the results of the static deflection tests where the bulk of the difference was attributed to the breadboard mount flexure actual thickness being less that the model thickness.

3.6 DYNAMIC RESPONSE TESTS - SINE SWEEP

OBJECTIVE:
The objectives of the sine sweep test are twofold: 1) To obtain additional natural frequency information, and 2) To check out all instrumentation and mounting hardware prior to performing a random vibration test.

PROCEDURE:
Accelerometers were mounted as shown in Figure 6. The mount assembly was attached to a shaker table and a sine sweep, in each of three orthogonal directions, was run at 0.1 G from 20 to 2000 Hz at a rate of 1 minute per octave.

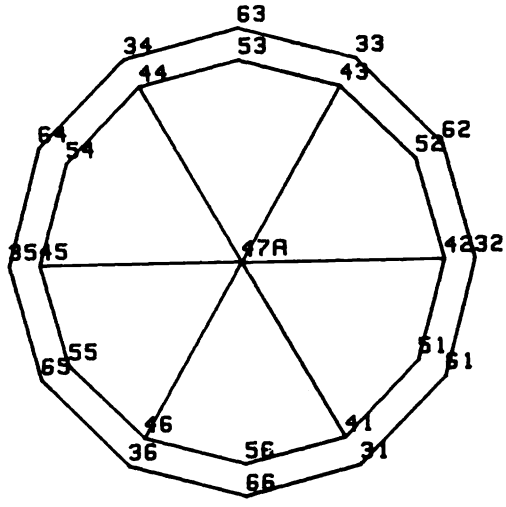

Figure 7 Modal Test Measurement Points

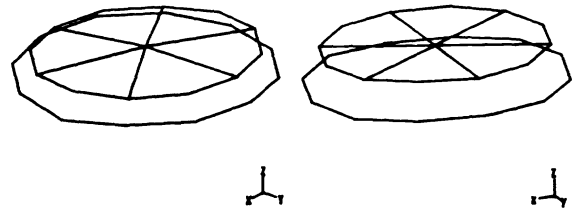

Left Test 244 Hz. Right Calculated 253 Hz.

Figure 8 Mode 1 Test and Analysis

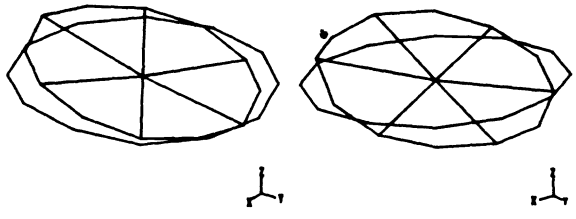

Left Test 309 Hz. Right Calculated 324 Hz.

Figure 9 Mode 2 Test and Analysis

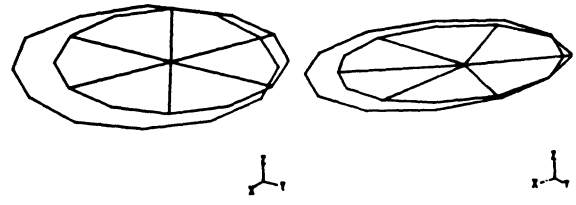

Left Test 557 Hz. Right Calculated 592 Hz.

Figure 10 Mode 3 Test and Analysis

RESULTS:

Table 7 gives the identified natural frequencies from the sine sweep tests. These data show that all three frequencies were 5-6% higher that the modal test frequencies, and closer to the predicted frequencies.

Figure 11 shows a typical sine sweep response curve. This plot shows that the resonance peaks were clearly defined.

3.7 DYNAMIC RESPONSE - RANDOM VIBRATION TESTS

OBJECTIVE:

There were three objectives to the dynamic response tests: 1) To measure the response of the optic for comparison against the calculated response amplitude, in order to calibrate the finite element models, especially the modeled damping, 2) To subject the assembly to specified vibration exposure and measure the change in alignment (tilt and decenter) as a result of that exposure, and 3) To determine if the random vibration exposure caused any damage to the assembly.

PROCEDURE:
The configuration of the assembly was identical to that used for the sine sweep test (See Figure 6). The first random vibration exposure was run at 5 Grms for one minute per axis for three orthogonal axes. The input spectrum was from 20 to 2000 Hz.

Following the first set of three exposures, the optic was removed from the vibration test facility and remounted on the alignment tower and tilt and decenter were measured with respect to the pre-vibration baseline. A second random vibration exposure was run at 7.5, 7.4 and 6.2 Grms for three minutes per axis for three orthogonal axes. Alignment was checked following this exposure. A third random vibration exposure test was conducted at 8.4 Grms for three minutes each for the three axes. Alignment was, again, measured against the original as-assembled tilt and decenter measurements.

RESULTS:
The results of the 8.4 Grms vibration exposure showed minimal and acceptable shifts in alignment. The results are shown in Table 3. The vibration amplitude results were in good agreement with the finite element predictions, as shown in Table 8. The most appropriate comparison is between the vector sum numbers for the prediction and measurement. Comparing the vector sum, rather than the individual components, removes the effects of accelerometer alignment.

VIBRATION AXIS	A AXIS		B AXIS		C AXIS	
	5.0 Grms	7.5 Grms	5.0 Grms	7.5 Grms	5.0 Grms	7.5 Grms
RADIAL						
TEST DATA	14.7	19.6	14.9	22.8	11.3	16.3
ANALYSIS	17.6	26.4	16.9	25.4	11.2	16.8
AXIAL						
TEST DATA	11.6	14.0	4.1	5.2	8.3	11.0
ANALYSIS	11.3	17.0	1.5	2.3	12.8	19.2
VECTOR SUM						
TEST DATA	18.7	24.1	15.1	23.4	14.0	19.7
ANALYSIS	20.9	31.4	17.0	25.1	17.0	21.1

Table 8 Dynamic Random Response

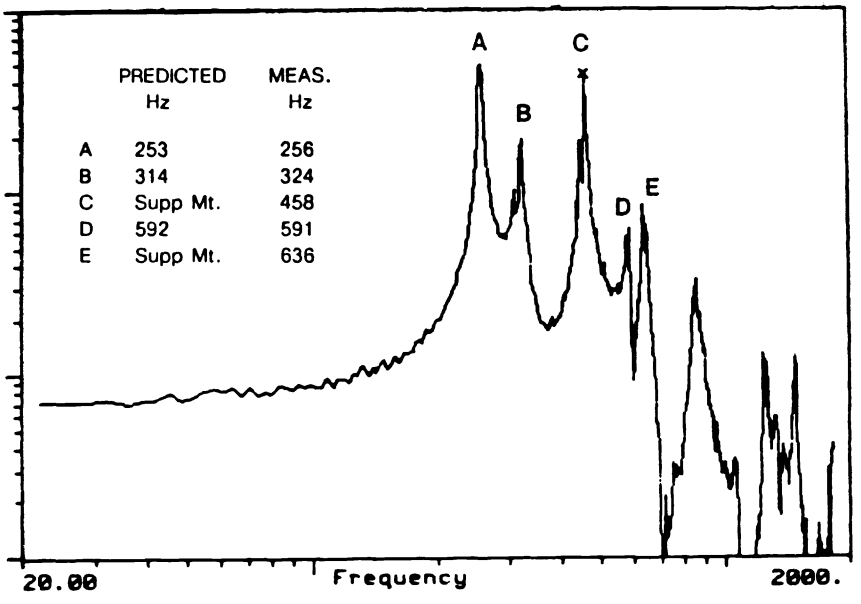

Figure 11 Typical Sine Sweep Response Curve

4. CONCLUSIONS

The results of the analyses and breadboard testing quantified the performance of the Integral Ring mount design concept across the complete range of operational environments. This data was valuable in facilitating a concurrent design effort on a full optical system, which used this optic mount concept in two locations. The breadboard program provided validated models and data for the full design and systems analyses. The breadboard effort also served as a pathfinder for the manufacturing
processes required for the assembly of these mounts in the full optical system. The mount design concept subsequently performed well in the full optical system. The Integral Ring design concept, with its supporting test data and analysis models could be readily scaled up to other optical systems with similar environmental and performance requirements.

5. REFERENCES

1) Vukobratovich, D, Introduction to Opto-Mechanical Design for Mechanical Engineers, SPIE Optical/Opto-Electronic Engineering Update series, 1988.

2) Yoder, P. R., Opto-Mechanical Systems Design, Marcel Dekker, New York, 1986.

3) Genberg, V. L., "Optical Surface Evaluation", SPIE Symposium on Structural Mechanics of Optical Systems, November 1983.

4) Genberg, V. L., Structural Analysis of Optics and Optical Systems, SPIE Technical Symposium, April 8, 1988